



## Analytical Study of Skew-cosh-Gaussian Laser Beam Propagation through Collisionless Plasma

K Y Khandale<sup>a</sup>, P T Takale<sup>a</sup>, S S Patil<sup>b</sup>, P P Nikam<sup>b</sup>, M B Mane<sup>b</sup>, S D Patil<sup>b\*</sup> & M V Takale<sup>a</sup>

<sup>a</sup>Department of Physics, Shivaji University, Kolhapur 416 004, India

<sup>b</sup>Department of Physics, Devchand College, Arjunnagar, Kolhapur 591 237, India

Received 11 October 2022; accepted 18 November 2022

In the present theoretical investigation the domains of the order of skew-cosh-Gaussian (skew-chG) laser beams for a given set of skewness parameters and its significant effect on the self-focusing/defocusing in collisionless plasma has been studied. The nonlinearity in the dielectric function of collisionless plasma is mainly due to the ponderomotive force. By following parabolic wave equation approach under Wentzel-Kramers-Brillouin (WKB) and paraxial approximations, nonlinear coupled differential equations are established for the beam width parameters. These equations have been solved numerically by using fourth-order Runge-Kutta method. The results obtained are presented graphically and discussed.

**Keywords:** Skew-cosh-Gaussian; Skewness parameters; Collisionless plasma; Self-focusing

### 1 Introduction

Plasma is a quasineutral gas of charged as well as neutral particles which exhibits collective behaviour. Self-focusing is a third order nonlinear optical phenomenon in which the intense laser beam incident on medium changes the optical properties in such a way that beam comes to focus within the medium. Self-focusing/defocusing of laser beams in nonlinear media has been extensively reviewed by Akhmanov *et al.*<sup>1</sup>. Sodha *et al.*<sup>2</sup> did its pedagogical straight forward extension to plasmas. There are three main mechanisms viz., collisional, relativistic and ponderomotive that contribute to modifications in the dielectric constant of plasma in the investigations of laser-plasma interaction<sup>2</sup>. The interaction of high-power laser beams with plasmas is not only of technological attention but also rich in various nonlinear phenomena which are crucial in so many applications, such as high harmonic generation<sup>3</sup>, soft x-ray generation<sup>4</sup>, ionospheric modification<sup>5</sup>, laser driven electron acceleration<sup>6</sup>, self-phase modulation<sup>7</sup>, fast ignition for inertial confinement fusion<sup>8</sup>, generation of new radiation sources<sup>9</sup> *etc.*

Collisionless plasma is weakly coupled. Particles in plasma interact through the Coulomb's force which reaches over a long distance. The long-range part of the Coulomb's potential is masked by the collective

behaviour of the particles and particles are interacting with the screened Coulomb's potential. When the intense laser beam propagates through collisionless plasma, the electrons in plasma are subjected to the ponderomotive force due to the gradient of the inhomogeneous irradiance. In the axial region, where the laser beam is more intense, ponderomotive force drives electrons away from it. As a result, expulsive force is generated within the channel, while plasma pressure outside the channel offsets the expulsive force, leading to decreased density inside the channel. In steady state, the effective dielectric constant is improved. Self-focusing and defocusing are caused by this self-induced inhomogeneity in the dielectric function of the plasma<sup>10</sup>. In past few decades, different kinds of laser beam profiles have been explored for the studies of propagation dynamics of laser beams. Few of them are cosh-Gaussian beams<sup>11-13</sup>, Hermite-Gaussian beams<sup>14</sup>, Hermite-cosh-Gaussian beams<sup>15-17</sup>, elegant Hermite-cosh-Gaussian beams<sup>18,19</sup>, Quadruple Gaussian beams<sup>20</sup>, Bessel-Gaussian beams<sup>21,22</sup>, finite Airy-Gaussian beams<sup>23</sup> *etc.*

Recently, skew-chG laser beam has attracted a remarkable attention due to its specific properties. Such beam can create wakefield and generate THz radiation<sup>24</sup>. It has been suggested that chG beam is useful for harmonic generation<sup>25</sup> and electron acceleration<sup>26</sup>. In the present work, the domains of the

\*Corresponding author: (E-mail: sdpatil\_phy@rediffmail.com)

order  $n$  of skew-chG laser beams have been investigated in collisionless plasma. By considering symmetry in two transverse directions of the beam, an electric field profile of skew-chG laser beam have been explored. It has been also emphasized that the order  $n$  and skewness parameter  $s$  of skew-chG laser beam plays an important role in the propagation dynamics of skew-chG laser beam. Furthermore, the analytical study in the present situation focuses exploration of order  $n$  and skewness parameter  $s$  of the skew-chG laser beam. To be more precise, present study investigates analytically the domains of the order  $n$  of skew-chG laser beam for given set of skewness parameter  $s$  so as to investigate its effect on propagation dynamics of the skew-chG laser beams. In Section 2, nonlinear coupled differential equations for beam-width parameters have been established for skew-chG laser beams in isotropic collisionless plasma. In section 3, numerical results are presented graphically and discussed. Finally, a brief conclusion is added in section 4.

**2 Basic Formulation**

The initial electric field profile of skew-chG laser beam in Cartesian co-ordinate system can be written as,

$$E(x, y, 0) = E_0 \cosh^n \left( \frac{s_x x}{r_0} \right) e^{\left( -\frac{x^2}{r_0^2} \right)} \cosh^m \left( \frac{s_y y}{r_0} \right) e^{\left( -\frac{y^2}{r_0^2} \right)} \dots (1)$$

where  $n$  and  $m$  are order of skewness,  $r_0$  is initial beam radius,  $E_0$  is amplitude at central position and  $s_x$  and  $s_y$  are skewness parameters along  $x$  and  $y$  directions respectively. For a convenience, we can express Eq. (1) as follows

$$E(x, y, 0) = \frac{E_0}{z^{(n+m)}} \exp \left( \frac{n^2 s_x^2}{4} \right) \exp \left( \frac{m^2 s_y^2}{4} \right) \left\{ \left[ e^{-\left( \frac{x}{\sqrt{n} r_0} + \frac{\sqrt{n} s_x}{2} \right)^2} + e^{-\left( \frac{x}{\sqrt{n} r_0} - \frac{\sqrt{n} s_x}{2} \right)^2} \right]^n \left[ e^{-\left( \frac{y}{\sqrt{m} r_0} + \frac{\sqrt{m} s_y}{2} \right)^2} + e^{-\left( \frac{y}{\sqrt{m} r_0} - \frac{\sqrt{m} s_y}{2} \right)^2} \right]^m \right\} \dots (2)$$

The collisionless plasma is described by the dielectric function which can be expressed as<sup>2</sup>

$$\epsilon = \epsilon_0 + \phi (EE^*), \dots (3)$$

where  $\epsilon_0$  and  $\phi (EE^*)$  represents the linear and nonlinear parts of dielectric function  $\epsilon$ , and  $\epsilon_0 = 1 - (\omega_p^2/\omega^2)$ , where  $\omega_p$  is the plasma frequency in the absence of the beam,  $\omega$  is the angular frequency of laser and  $\omega_p = \sqrt{4\pi N_0 e^2/m_0}$ , where  $N_0$ ,  $e$  and  $m_0$

are the density of plasma electrons in the absence of the beam, charge on electron and rest mass of electron respectively. The term  $\phi (EE^*)$  exhibit saturation behaviour with  $EE^*$  and for collisionless plasma, it may be expressed as<sup>2</sup>,

$$\phi (EE^*) = \frac{\omega_p^2}{\omega^2} \left[ 1 - \exp \left( -\frac{3 m_0 \alpha EE^*}{4 M} \right) \right] \dots (4)$$

with  $\alpha = e^2 M/6 k_B T_0 \omega^2 m_0^2$ , where  $k_B$ ,  $T_0$  and  $M$  are Boltzmann's constant, equilibrium plasma temperature and mass of ion respectively. The wave equation governing the electric field of the laser and dielectric function  $\epsilon$  of the plasma can be expressed as

$$\nabla^2 E - \frac{\epsilon}{c^2} \frac{\partial^2 E}{\partial t^2} = 0 \dots (5)$$

In writing Eq. (5), the term  $\nabla(\nabla \cdot E)$  has been neglected, which has been justified when  $(c^2/\omega^2) \left| \frac{1}{\epsilon} \nabla^2 \ln \epsilon \right| \ll 1$ . In WKB approximation solution of Eq. (5) can be written as follows

$$E = A(x, y, z) \exp [i(\omega t - kz)] \dots (6)$$

Substituting  $\epsilon$  and  $E$  from Eqs. (3) and (6) in Eq. (5) and solving, one can obtain

$$\frac{\partial^2 A}{\partial x^2} + \frac{\partial^2 A}{\partial y^2} + \frac{\omega^2}{c^2} \phi (EE^*) A = 2ik \frac{\partial A}{\partial z} \dots (7)$$

To solve parabolic wave Eq. (7), we now express  $A(x, y, z)$  as

$$A(x, y, z) = A_0(x, y, z) \exp[-ikS(x, y, z)] \dots (8)$$

where,  $A_0(x, y, z)$  and  $S(x, y, z)$  are real functions of  $x$ ,  $y$  and  $z$  and  $S$  is the eikonal of the beam. Substituting for  $A$  from Eq. (8) in Eq. (7) and equating real and imaginary parts, we get

$$2 \left( \frac{\partial S}{\partial z} \right) + \left( \frac{\partial S}{\partial x} \right)^2 + \left( \frac{\partial S}{\partial y} \right)^2 = \frac{1}{k^2 A_0} \left( \frac{\partial^2 A_0}{\partial x^2} + \frac{\partial^2 A_0}{\partial y^2} \right) + \frac{\phi}{\epsilon_0} (A_0 A_0^*) \dots (9)$$

and

$$\frac{\partial A_0^2}{\partial z} + \left( \frac{\partial S}{\partial x} \right) \left( \frac{\partial A_0^2}{\partial x} \right) + \left( \frac{\partial S}{\partial y} \right) \left( \frac{\partial A_0^2}{\partial y} \right) + \left( \frac{\partial^2 S}{\partial x^2} + \frac{\partial^2 S}{\partial y^2} \right) A_0^2 = 0 \dots (10)$$

Following the approach given by Akhmanov *et al.*<sup>1</sup> and its extension by Sodha *et al.*<sup>2</sup>, the solutions of the Eqs. (9) and (10) can be written as

$$S = \beta_1(z) \frac{x^2}{2} + \beta_2(z) \frac{y^2}{2} + \phi(z) \dots (11)$$

and

$$A_0^2(x, y, z) = \frac{E_0^2}{4^{(n+m)} f_1(z) f_2(z)} \exp \left( \frac{n^2 S_x^2}{2} \right) \exp \left( \frac{m^2 S_y^2}{2} \right) \left\{ \left( \exp \left[ -2 \left( \frac{x}{\sqrt{n} f_1(z) r_0} - \frac{\sqrt{n} s_x}{2} \right)^2 \right] + \exp \left[ -2 \left( \frac{x}{\sqrt{n} f_1(z) r_0} + \frac{\sqrt{n} s_x}{2} \right)^2 \right] \right)^n + 2 \exp \left[ -\left( \frac{2x^2}{n r_0^2 f_1(z)^2} + \frac{n^2 s_x^2}{2} \right) \right] \right\} \left\{ \left( \exp \left[ -2 \left( \frac{y}{\sqrt{m} f_2(z) r_0} - \frac{\sqrt{m} s_y}{2} \right)^2 \right] + \exp \left[ -2 \left( \frac{y}{\sqrt{m} f_2(z) r_0} + \frac{\sqrt{m} s_y}{2} \right)^2 \right] \right)^m + 2 \exp \left[ -\left( \frac{2y^2}{m r_0^2 f_2(z)^2} + \frac{m^2 s_y^2}{2} \right) \right] \right\}$$

... (12)

where  $\beta_1(z) = (1/f_1)(\partial f_1(z)/\partial z)$  and  $\beta_2(z) = (1/f_2)(\partial f_2(z)/\partial z)$ , here,  $\beta_1(z)$  and  $\beta_2(z)$  are the inverse of the radius of curvature of the beam along  $x$  and  $y$  directions respectively,  $\phi(z)$  is the axial phase,  $f_1(z)$  and  $f_2(z)$  are dimensionless beam-width parameters along  $x$  and  $y$  directions of the beam respectively. Substituting Eqs. (11) and (12) in Eq. (9), we have obtained differential equations for  $f_1$  and  $f_2$  of skew-chG laser beams as

$$\frac{d^2 f_1}{d\xi^2} = \frac{n^2 s_x^4 - n s_x^4 - 4 n s_x^2 + 4}{f_1^3} - \frac{3 m_0 \alpha E_0^2 e^{-\frac{3 m_0 \alpha E_0^2}{4 M f_1 f_2}} (2 - n s_x^2) r_0^2 \omega_p^2}{4 M f_1^2 f_2 c^2} \quad \dots (13)$$

and

$$\frac{d^2 f_2}{d\xi^2} = \frac{n^2 s_y^4 - n s_y^4 - 4 n s_y^2 + 4}{f_2^3} - \frac{3 m_0 \alpha E_0^2 e^{-\frac{3 m_0 \alpha E_0^2}{4 M f_1 f_2}} (2 - n s_y^2) r_0^2 \omega_p^2}{4 M f_2^2 f_1 c^2} \quad \dots (14)$$

where  $\xi = z/R_d$  is the dimensionless distance of propagation and  $R_d = k r_0^2$  is the Rayleigh length with  $k = (\omega/c)\sqrt{\epsilon_0}$  as wave number. Now, we have made analytical investigation by considering the same order of skewness i.e.,  $n = m$  as well as skewness parameters  $s_x = s_y = s$  along  $x$  and  $y$  directions respectively. Eqs. (13) and (14) are nonlinear coupled differential equations that shows the variation of the  $f_1$  and  $f_2$  with respect to the dimensionless distance of propagation  $\xi$ . The first term on the right-hand side of these equations leads to the diffraction divergence which is responsible for defocusing and the second term leads to convergence resulting from the ponderomotive nonlinearity which is responsible for self-focusing. The beam gets self-trapped, when the self-focusing and diffraction of a laser beam are perfectly balanced.

### 3 Results and Discussion

By applying initial conditions on Eqs. (13) and (14),  $f_1(\xi = 0) = f_2(\xi = 0) = 1$  and  $d^2 f_1/d\xi^2 = d^2 f_2/d\xi^2 = 0$  considering the symmetry such as  $s_x = s_y = s$ , and  $n = m$  we get the expression for dimensionless critical beam radius  $\rho_0 = \omega_p r_0/c$  in terms of critical intensity parameter  $p_0 = \alpha E_0^2$ , skewness parameter  $s$  and order of skewness  $n$  as

follows:

$$\rho_0 = \sqrt{\frac{4 M (n^2 s^4 - n s^4 - 4 n s^2 + 4)}{3 m_0 e^{-\frac{3 m_0 p_0}{4 M}} p_0 (2 - n s^2)}} \quad \dots (15)$$

Now, Eq. (15) can also be written as,

$$\frac{1}{\rho_0^2} = \frac{3 m_0 e^{-\frac{3 m_0 p_0}{4 M}} p_0 (2 - n s^2)}{4 M (n^2 s^4 - n s^4 - 4 n s^2 + 4)} \quad \dots (16)$$

For the maximum value of right-hand side we can write the Eq. (16) as

$$\frac{d}{dp_0} \left[ \frac{3 m_0 e^{-\frac{3 m_0 p_0}{4 M}} p_0 (2 - n s^2)}{4 M (n^2 s^4 - n s^4 - 4 n s^2 + 4)} \right] = 0 \quad \dots (17)$$

Solving the Eq. (17), one can obtain value of  $p_0$  at minimum value of  $\rho_0$  denoted as  $\rho_{0min}$ . Therefore, we can obtain

$$\rho_{0min} = \frac{2.7183 (n^2 s^4 - n s^4 - 4 n s^2 + 4)}{(2 - n s^2)} \quad \dots (18)$$

Equation (18) is used for further graphical and analytical explorations as discussed below. The expression of  $\rho_{0min}$  is purely dependent on skewness parameter  $s$  and order of skewness  $n$ . In Fig. 1, the variation of  $\rho_{0min}$  with order of skewness  $n$  for the given set of values of skewness parameters  $s$  (0.5, 1.0, 1.5, and 2.0) gives the domains of order of skewness  $n$ . The subsequent analytical investigation using Eq. (18), under the condition  $\rho_{0min} > 0$  results in four distinct domains corresponding to each value of skewness parameter  $s$ . The critical curve analysis results in clear discrimination of supercritical (above critical curve) and subcritical (below critical curve) regions. These two regions are always separated by

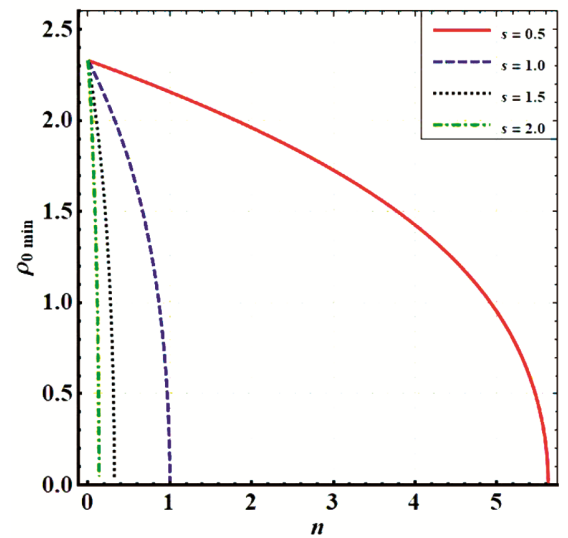


Fig. 1 — Domains of order  $n$  of skew-chG laser beams for given skewness parameter  $s$ .

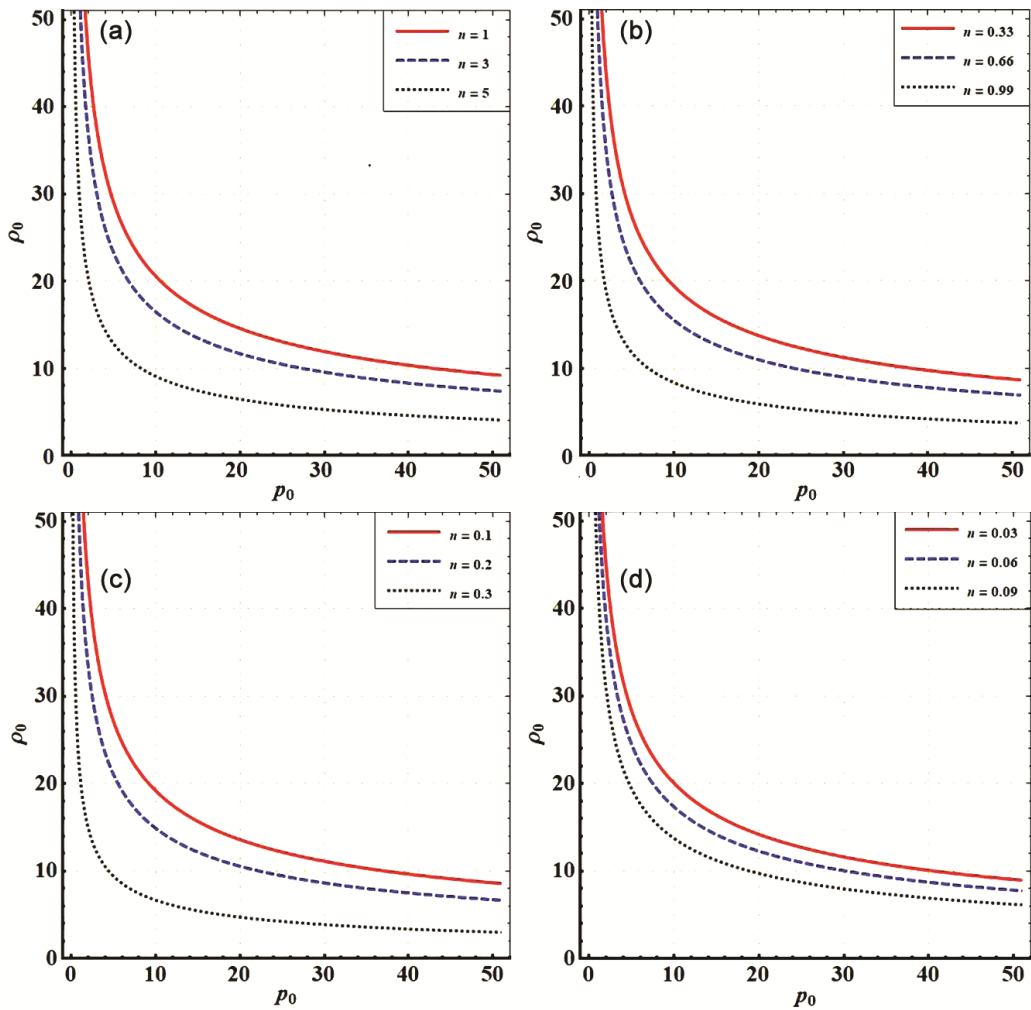


Fig. 2 — Critical curves for distinct values of skewness parameters  $s$  and same order of skewness (symmetry)  $n = m$  (a)  $s = 0.5$ , (b)  $s = 1.0$ , (c)  $s = 1.5$  and (d)  $s = 2.0$ .

critical curve. Thus, using Eq. (15), the Fig. 2 gives four sets of plots of critical curves where each set corresponds to given value of skewness parameter  $s$ . In those sets, in general, it is observed that with increase in the value of  $n$ , the critical curve shifts downward and saturates at its minimum value. For a point  $(\rho_0, p_0)$  in supercritical region, self-focusing is observed and for a point  $(\rho_0, p_0)$  in subcritical region, defocusing is observed. But for any point  $(\rho_0, p_0)$  on the critical curve, self-trapping of skew-chG laser beam is obviously self-explanatory.

Finally, Eqs. (13) and (14) are solved numerically for the values of  $\rho_0 = 20.00$  (supercritical region),  $\rho_0 = 1.5550$  (subcritical region) and  $p_0 = 2448$  which are consistent with all the plots of critical curves in Fig. 2.

In Fig. 3 we have shown explicitly the variation of  $f_1$  and  $f_2$  with respect to the dimensionless distance of propagation  $\xi$ , for different domains of the order of skew-chG laser beam as shown in Table 1 along with  $\rho_0 = 20.00$  and  $\rho_0 = 1.550$  with  $p_0 = 2448$ .

The variations in  $f_1$  and  $f_2$  with respect to the domains of  $n$  are clearly evident in Fig. 3. We have taken the two different values of  $\rho_0 = 20.00$  and  $\rho_0 = 1.550$  which lives in supercritical and subcritical regimes respectively with  $p_0 = 2448$ . For  $\rho_0 = 20.00$  and  $p_0 = 2448$ , the self-focusing and for  $\rho_0 = 1.550$  and  $p_0 = 2448$  the steady defocusing of the skew-chG laser beams is noticed. For any value of  $\rho_0$  on the critical curve, the self-trapping of skew-chG laser beam observed which is

obviously self-explanatory. In addition, for the given skewness parameter  $s$  with respect to domains of orders of skew-chG laser beam  $n$  the rate of defocusing decreases. Also Fig. 3 depicts that when the domains of  $n$  increases with  $s$ , the self-focusing length decreases.

skewness parameter. For supercritical (subcritical) region, increase in rate of self-focusing (defocusing) is observed with increase in order of skew-chG laser beam for a given skewness parameter. As obvious, due to symmetry in two transverse directions  $n = m$ ,

Table 1 — Domains of order  $n$  of skew-chG laser beam for given set of skewness parameter  $s$ .

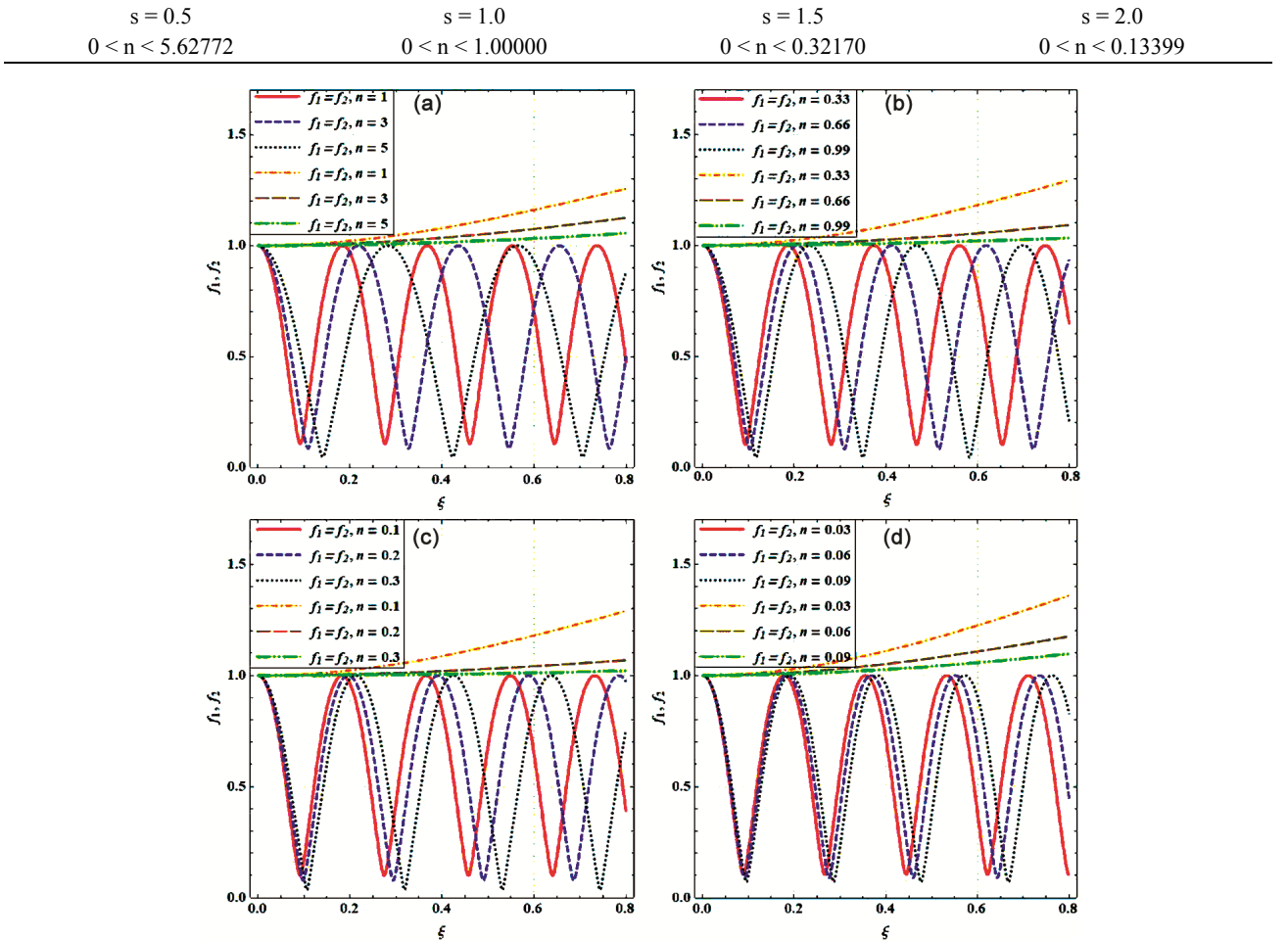


Fig. 3 — Variation of beam width parameters  $f_1$  and  $f_2$  with dimensionless distance of propagation  $\xi$  with  $p_0 = 2448$  for distinct skewness parameters  $s$  and domains of order  $n$  of skew-cosh Gaussian laser beams for  $\rho_0 = 20.00$  (self-focusing),  $\rho_0 = 1.5550$  (defocusing), (i)  $s = 0.5$  and  $0 < n < 5.62772$ , (ii)  $s = 1.0$  and  $0 < n < 1.00000$ , (iii)  $s = 1.5$  and  $0 < n < 0.32170$  and (iv)  $s = 2.0$  and  $0 < n < 0.13397$ .

#### 4 Conclusions

In conclusion, nonlinear coupled differential equations in transverse dimensions of the skew-chG beams are established using the parabolic wave equation approach under WKB and paraxial approximations. It is found that the domains of order of skew-chG laser beams decreases with increase in

$f_1$  and  $f_2$  shows perfect synchronisation.

#### Acknowledgement

The authors are thankful to UGC DSA-Phase-2 and DST-PURSE Phase-2, (2018-2023) plan for giving computational research facilities in Department of Physics, Shivaji University, Kolhapur, India.

#### References

- 1 Akhmanov S A, Sukhorukov A P & Khokhlov R V, *Sov Phy Usp*, 10 (1968) 609.
- 2 Sodha M S, Ghatak A K & Tripathi V K, *Prog Opt*, 13 (1976) 169.
- 3 Kant N & Thakur V, *Optik*, 127 (2016) 4167.
- 4 Bartnik A, *Opto-Electron Rev*, 23 (2015) 172.
- 5 Guzdar P N, Chaturvedi P K, Papadopoulos K & Ossakow S L, *J Geophys Res*, 103 (1998) 2231.
- 6 Ghotra H S & Kant N, *Opt Commun*, 383 (2017) 169.
- 7 Giulietti A & Giulietti D, *J Plasma Phys*, 81 (2015) 49581060.
- 8 Betti R & Hurricane O A, *Nat. Phys*, 12 (2016) 717.
- 9 Jaroszynski D A & Vieux G, *AIP Conf Proc*, 647 (2012) 902.
- 10 Sodha M S, Prasad S & Tripathi V K, *J Appl Phys*, 46 (1975) 637.
- 11 Vhanmore B D, Patil S D, Valkunde A T, Urunkar T U, Gavade K M & Takale M V, *Laser Part Beams*, 35 (2017) 670.
- 12 Urunkar T U, Patil S D, Valkunde A T, Vhanmore B D, Gavade K M & Takale M V, *Laser Part Beams*, 36 (2018) 254.
- 13 Urunkar T U, Patil S D, Valkunde A T, Vhanmore B D, Gavade K M & Takale M V, *Commun Theor Phys*, 70 (2018) 220.
- 14 Takale M V, Navare S T, Patil S D, Fulari V J & Dongare M B, *Opt Commun*, 282 (2009) 3157.
- 15 Patil S D, Takale M V, Navare S T, Fulari V J & Dongare M B, *J Opt*, 36 (2007) 136.
- 16 Patil S D, Takale M V, Navare S T & Dongare M B, *Laser Part Beams*, 28 (2010) 343.
- 17 Wani M A & Kant N, *Optik*, 127 (2016) 4705.
- 18 Vhanmore B D, Valkunde A T, Urunkar T U, Gavade K M, Patil S D & Takale M V, *Eur Phys J D*, 73 (2019) 45.
- 19 Vhanmore B D, Takale M V & Patil S D, *Phys Plasmas*, 27 (2020) 063104.
- 20 Vij S & Aggarwal M, *Commun Theor Phys*, 70 (2018) 317.
- 21 Patil S D, Vhanmore B D & Takale M V, *J Opt*, 49 (2020) 510.
- 22 Patil S D, Vhanmore B D & Takale M V, *J Russ Laser Res*, 42 (2021) 45.
- 23 Nikam P P, Pawar V S, Takale P T, Khandale K Y, Patil S S, Mane M B, Patil S D & Takale M V, *Indian J Pure Appl Phys*, 60 (2022) 576.
- 24 Singh D, Malik H K & Nishida Y, *Euro Phy. Lett*, 127 (2019) 55001.
- 25 Sharma V, Thakur V & Kant N, *Opt Quant Electron*, 52 (2020) 444.
- 26 Singh J, Rajput J, Ghotra H S & Kant N, *Commun Theor Phys*, 73 (2021) 095502.